Transverse momentum dependence of dileptons from parton matter produced in ultrarelativistic heavy-ion collisions

B. Kämpfer[1,2] and O.P. Pavlenko[1,3]
[1]*Research Center Rossendorf, Institute for Nuclear and Hadron Physics, PF 51 01 19, 01314 Dresden, Germany*
[2]*Institute of Theoretical Physics (KAI e.V.), Technical University Dresden, Germany*
[3]*Institute of Theoretical Physics, Kiev, Ukraine*
(Received 1 March 1993; revised manuscript received 7 October 1993)

The $M_\perp$ scaling property of the dilepton spectrum from early parton matter in ultrarelativistic heavy collisions is analyzed for various mechanisms of initial parton production. If there is no essentially additional scale in the parton distribution, we find even for strong off-equilibrium parton matter approximate scaling, while such scales as low-momentum cutoff or parton masses cause strong scaling violations.

PACS number(s): 25.75.+r, 12.38.Mh, 24.85.+p

I. INTRODUCTION

Dileptons are considered a useful tool to investigate the dynamics and the state of matter in the course of ultrarelativistic heavy-ion collisions. In particular, the lepton pairs are thought to represent direct messengers from the early stages where the transient creation of deconfined matter is prejudiced [1–3]. Whether the energy density and lifetime are large enough to achieve a locally equilibrated quark-gluon plasma is a question to be decided experimentally. The presently available estimates and simulation codes predict the possibility of creating deconfined parton matter in future experiments at the Relativistic Heavy Ion Collider (RHIC) in Brookhaven.

In general the dilepton spectrum $dN/dM_\perp^2 dq_\perp^2 dY$, as a function of the transverse mass of the pair $M_\perp = \sqrt{M^2+q_\perp^2}$ (M is the invariant mass, and $q_\perp$ the transverse momentum, while Y denotes the rapidity) and transverse momentum, depends separately on both $M_\perp$ and $q_\perp$ at fixed Y. Integrating over $q_\perp$ one gets the commonly studied mass spectrum dN/dM^2dY [3] that is particularly suitable to get information on the initial temperature T_0 of a quark-gluon plasma due to the essential dependence $dN/dM^2dY \propto T_0^6 \exp(-M/T_0)$. The existence of other, i.e., conventional, processes for creating lepton pairs makes it, however, difficult to identify unambiguously the quark-gluon plasma formation when using only the above mass spectrum. In this situation the detailed information of the full spectrum $dN/dM_\perp^2 dq_\perp^2 dY$ is expected to allow for a more sensible diagnostic.

As pointed out in Refs. [4–6] under certain conditions the dilepton yield from a locally equilibrated quark-gluon plasma depends only on the transverse mass, i.e., $dN/dM_\perp^2 dq_\perp^2 dY \propto F(M_\perp)$; that is, it scales with $M_\perp$. In a recent paper [7] this property has been proposed to be used as a unique signature of the formation of a quark-gluon plasma. In particular, the yield from hadron matter is shown to display strong violation of the scaling. Hence the authors of Ref. [7] conclude that at conditions to be expected at RHIC concerning the multiplicities of secondary charged particles dN_c/dy, the dilepton yield from quark-gluon plasma dominates in the continuum region around J/ψ over the hadron gas and a possible mixed phase, and as result one should observe the $M_\perp$ scaling. In opposite case, if strong violations of the $M_\perp$ scaling would be observed, a quark-gluon plasma had not been created.

The conditions of the $M_\perp$ scaling are (i) predominant longitudinal boost-invariant matter flow, (ii) local equilibration (thermalization), and applicability of the Boltzmann approximation, and (iii) no scale other than the temperature T, and the lepton masses can be neglected. Any other essential scale or new parameter violates the scaling; e.g., in the hadron gas and a possible mixed phase the electromagnetic π form factor (described by ρ mass and width) causes such a scaling violation. Also transverse expansion is a scaling violating in the same direction, in particular in the confined phase [7,8]. The scaling violation by higher-order QCD processes is discussed in Ref. [5] (cf. also [7]).

In the present paper we would like to extend the approach of Ref. [7] and also include preequilibrium parton matter. Preequilibrium parton matter has been considered previously, e.g in Ref. [9], and Refs. [10,11] in the collisionless regime. It is quite obvious that the partonic matter needs some time to evolve from the overlapping nuclear distributions towards a locally thermalized state. It might be suspected that the early stages just give a substantial contribution to the dilepton yield, or even might dominate it. Estimates of the Drell-Yan contribution [12], which is considered as a rather unspectacular signal from the primary parton collisions, show that under unfavorable conditions this contribution could dominate the continuum in the J/ψ region and above. Parton kinetics estimates [13–15] show that, for RHIC conditions, preequilibrium parton matter might shine brighter than the subsequent equilibrium matter. This is supported by recent parton cascade calculations [16]. Also the very strong dependence of the plasma yield on the initial temperature [3] is a hint on the importance of early stages despite their short lifetime.

Here we study possible origins of the $M_\perp$ scaling vio-

lation of the dilepton spectrum from preequilibrium parton matter in a kinetic framework. We show in line with Ref. [11] that under certain conditions strong off-equilibrium parton matter displays approximate scaling, as also the Drell-Yan contribution does at $M_\perp > 2$ GeV [7,11]. Otherwise we find that the inclusion of essentially additional parameters, such as a low-momentum cutoff and parton masses, give rise to a noticeable violation of scaling. Strong scaling violations have been observed in the ambitious parton cascade simulations [17] and are there attributed to higher twist effects which cause effective parton masses and form factors. Whether this scaling violation is a generic effect and how it depends on model parameters, like the low-momentum cutoff for the applicability of perturbative cross sections, is not yet obvious. Our kinetic approach is based on a transparent analytical model, so that we hope to present a complementary study to the numerically involved simulations [17] in order to provide a better physical understanding of the strength of the $M_\perp$ scaling violation on model parameters and assumptions.

II. PARTON KINETICS AND DILEPTON YIELD

The propositions we rely on are as follows.

(i) Boost-invariant longitudinal flow of matter, i.e., the four-volume can be written as $d^4x = d\tau\tau d\eta d^2r$ with $\tau = \sqrt{t^2 - z^2}$ as proper time, and $\eta = \frac{1}{2}\ln(t+z)/(t-z)$ as space-time rapidity, and d^2r as transverse area, and any quantity is independent of η. The four-velocity of matter is then $u^\mu = (\cosh\eta, \sinh\eta, \mathbf{0})$.

(ii) Applicability of kinetic theory for the dilepton rate

$$\frac{dN}{d^4x d^4Q} = \int \frac{d^3p_1}{(2\pi)^3}\frac{d^3p_2}{(2\pi)^3} f(x,p_1) f(x,p_2) \times v\sigma(M^2)\delta^{(4)}(Q - p_1 - p_2) \tag{1}$$

with the pair four-momentum $Q^\mu = (M_\perp \cosh Y, M_\perp \sinh Y, \mathbf{q}_\perp)$ and the relative parton velocity $v = \frac{M^2}{2E_1E_2}\sqrt{1 - \frac{4m_q^2}{M^2}}$ and the quark fusion cross section into a pair $\sigma(M^2) = \frac{4\pi\alpha^2}{3M^2}\frac{20}{3}\sqrt{1 - \frac{4m_q^2}{M^2}}$ ($\alpha = \frac{1}{137}$, and m_q is the quark mass). The use of the perturbative cross section $q\bar{q} \to l\bar{l}$ as a dominant dilepton channel is supported by Ref. [16], even in a lack of chemically equilibrated quarks as in the hot glue scenario [18].

(iii) The single-particle distribution function f obeys a kinetic equation of Boltzmann type, $p^\mu \partial_\mu f = C$. We employ for the collision term the relaxation-time approximation $C = -\tau_{\rm rel}^{-1} u^\mu p_\mu (f - f_{\rm eq})$ with the relaxation time $\tau_{\rm rel}$, parton four-momentum $p^\mu = (m_\perp \cosh y, m_\perp \sinh y, \mathbf{p})$ where $m_\perp = \sqrt{p_\perp^2 + m_q^2}$, and fiducial matter four-velocity u^μ for the reference distribution function $f_{\rm eq} = \exp[-u^\mu p_\mu / T(\tau)]$ needed for linearizing the collision term [13,19].

The dilepton yield might then be cast into the form

$$\frac{dN}{dM_\perp^2 dq_\perp^2 dY} = \frac{5\alpha^2 R^2}{72\pi^3}\int_{\tau_0}^{\tau_f} d\tau\tau J(f,\bar{f}), \tag{2}$$

$$J = \int_{-\infty}^{\infty} d\eta \int_{-\infty}^{\infty} d\xi_1 \int_{m_\perp^-}^{m_\perp^+} \frac{dm_{\perp 1} m_{\perp 1} f(m_{\perp 1}, \xi_1, \tau)\bar{f}(m_{\perp 2}, \xi_2, \tau)}{[(m_{\perp 1}^2 - m_q^2)q_\perp^2 - (M_\perp m_{\perp 1}\cosh(\eta - \xi_1) - \frac{1}{2}M^2)]^{1/2}},$$

$$\xi_{1,2} = \eta - y_{1,2}, \quad m_{\perp 2} = \sqrt{M_\perp^2 - 2m_{\perp 1}M_\perp \cosh(\eta - \xi_1) + m_{\perp 1}^2}, \tag{3}$$

$$\sinh\xi_2 = m_{\perp 2}^{-1}(M_\perp \sinh\eta - m_{\perp 1}\sinh\xi_1),$$

$$m_\perp^\pm = \frac{M^2 M_\perp \cosh(\eta - \xi_1) \pm q_\perp \sqrt{M^4 - 4m_q^2[M_\perp^2 \cosh^2(\eta - \xi_1) - q_\perp^2]}}{2[M_\perp^2 \cosh^2(\eta - \xi_1) - q_\perp^2]}.$$

In the limiting case of large relaxation time $\tau_{\rm rel} \gg \tau_{0,f}$ the distribution function is described essentially by the free-stream solution

$$f(m_\perp, \xi, \tau) = f_0(m_\perp, \xi_0), \tag{4}$$

where $f_0(m_\perp, \xi) \equiv f(m_\perp, \xi, \tau_0)$ is the initial distribution, and $\xi_0 = \operatorname{arcsinh}(\frac{\tau}{\tau_0}\sinh\xi)$ (for the general solution see [13,19]). The studies [8] demonstrate that the transverse expansion has little influence on the short-living deconfined phase. Therefore we neglect here dynamical transverse degrees of freedom and use a homogeneous transverse distribution.

To draw conclusions from Eq. (2) one has to know the parton distribution f. This is given by Eq. (4) in the free-stream approximation or by the more involved solution of the kinetic basic equation. Such kinetic equations represent initial value problems. Therefore one must specify $f(\tau_0)$. The linearized kinetic theory version is probably not applicable for rapid changes of f which are expected in the very early evolution when the secondaries are produced. We therefore leave out this ignition stage and

follow the evolution after some finite "initial" time τ_0. According to the estimates in Ref. [15] this is the moment when the entropy is essentially produced.

We consider here three different initial distributions which are suggested by various simulations. The first one, which is called "soft," is related to Schwinger's mechanism of pair production in a strong external color flux tube [10,11], while the second one, which is named "semihard," is motivated by the perturbative QCD analysis of minijet production [20]. A third one is also based on improved semihard QCD calculations within the HIJING model [21], which show that the early parton distribution passes through an isotropic, nearly thermalized state. These initial distributions are

$$f_0(p_\perp,\xi)=\begin{cases}\mathcal{N}_1\exp(-p_\perp^2/K)\delta(\xi), & (5a)\\ \mathcal{N}_2 p_\perp^{-l}\Theta(p_\perp-p_\perp^*)\delta(\xi), & (5b)\\ \exp(-\frac{p_\perp\cosh(\xi)}{T_0}), & (5c)\end{cases}$$

($\xi=\eta-y$) where $\mathcal{N}_{1,2}$ are normalizations so that the energy density corresponds to an ideal gas with degeneracy 37 and temperature T_0 [$\mathcal{N}_1=24T_0^4/K^2$, $\mathcal{N}_2=12(l-4)(p_\perp^*)^{l-4}T_0^4$]; K in (5a) parametrizes the averaged transverse parton momentum $\langle p_\perp^2\rangle=\frac{\pi}{4}K$, which is estimated as 0.6 GeV^2 at the CERN Super Proton Synchrotron energies and is expected to increase to about 1 GeV^2 at RHIC, while $p_\perp^*$ in (5b) is the low-momentum cutoff, below this one the perturbative QCD parton cross sections are no longer applicable. The estimates in Ref. [20] indicate that at RHIC about half of the transverse energy of produced particles comes from the minijets, which give rise to the power-law distribution (5b) with $l\approx 7$. Otherwise, the HIJING simulations show, also for RHIC, a distribution as (5c) at a somewhat later time. Clearly, the distribution (5a) accounts for the soft processes which are realized even later. Probably Eq. (5b) is most appropriate at LHC energies where the semihard initial parton scatterings might dominate. The δ functions in Eqs. (5a) and (5b) reflect the fact that due to the mapping of configuration space and momentum space only particles with a certain momentum are scattered into a small volume element, and at early times a longitudinal momentum spreading did not yet evolve.

III. SLOW RELAXATION

Now we consider the limiting case of slow relaxation, when the solution (4) for the evolution of the parton distribution f applies. This case might be considered as a useful approximation of the dynamics near to τ_0. In the next section we also consider relaxation processes. The given free-stream approximation allows for analytical solutions of the integrals in the rate (2), and this makes this limiting case quite transparent.

Direct integration in Eq. (2) with (4) and (5) and $m_q=0$ results in

$$\frac{dN}{dM_\perp^2dq_\perp^2dY}=\begin{cases}\frac{5\alpha^2}{9\pi^4R^2}\left(\frac{dN_c}{dy}\frac{T_c}{K^2}\right)^2\ln\left(\frac{dN_c/dy}{3\pi R^2T_c^3\tau_0}\right)\exp\{-\frac{2M_\perp^2+q_\perp^2}{4K}\}\varphi(M_\perp,q_\perp,K), & (6a)\\ \frac{10\alpha^2}{9\pi^5R^2}\left((l-4)(p_\perp^*)^{l-4}T_c\frac{dN_c}{dy}\right)^2\ln\left(\frac{dN_c/dy}{3\pi R^2T_c^3\tau_0}\right)\frac{L(M_\perp,q_\perp,p_\perp^*)}{M_\perp\sqrt{M_\perp^2-q_\perp^2}}, & (6b)\\ \frac{5\alpha^2R^2\tau_0^2}{18\pi^3}\ln\left(\frac{\tau_f}{\tau_0}\right)I(M_\perp,q_\perp,T_0), & (6c)\end{cases}$$

with

$$\varphi=\frac{(2M_\perp^2-q_\perp^2)I_0(\frac{q_\perp^2}{4K})+q_\perp^2I_1(\frac{q_\perp^2}{4K})}{M_\perp\sqrt{m_\perp^2-q_\perp^2}},$$

where the $I_{0,1}$ are Bessel functions, and

$$L=\begin{cases}\int_{p_\perp^*(M_\perp-p_\perp^*)}^{M_\perp^2/4}\frac{dx}{x^{l-1}\sqrt{x-\frac14(M_\perp^2-q_\perp^2)}\sqrt{\frac14M_\perp^2-x}} & \text{for } q_\perp>M_\perp-2p_\perp^*,\\ \sum_{k=0}^{l-2}\binom{l-2}{k}\frac{B(k+\frac12,l-k-\frac32)}{M_\perp^{2k+1}(M_\perp^2-q_\perp^2)^{l-k-3/2}}2^{2(l-1)} & \text{for } q_\perp\le M_\perp-2p_\perp^*,\end{cases}$$

with the beta function B, and

$$I\approx\int_{x_-}^{x_+}dx\,x\frac{K_1\left(\frac{\sqrt{M_\perp^2-q_\perp^2}}{T_0}x\right)K_1\left(\frac{\sqrt{M_\perp^2-q_\perp^2}}{T_0}\left[\frac{M_\perp}{\sqrt{M_\perp^2-q_\perp^2}}-x\right]\right)}{\sqrt{x\left(\frac{M_\perp}{\sqrt{M_\perp^2-q_\perp^2}}-x\right)-\frac14}},\quad x_\pm=\frac{M_\perp\pm q_\perp}{2\sqrt{M_\perp^2-q_\perp^2}},$$

with K_1 as a modified Bessel function. In deriving Eqs. (6a)–(6c) we used the fact that for the initial conditions (5a) and (5b) the energy density evolves as $e=e_0(\tau_0/\tau)$, i.e., $T_c=T_0(\frac{\tau_0}{\tau_f})^{1/4}$, while for (5c) the freeze-out conditions are given by the relation $\frac{\tau_0}{\tau_f}h(\frac{\tau_0}{\tau_f})=(\frac{T_c}{T_0})^4$, $h(x)=\frac12(x+\frac{\arcsin\sqrt{1-x^2}}{\sqrt{1-x^2}})$; that gives us the final time τ_f at fixed values of T_c, dN_c/dy, and τ_0. Remember that in the present free-stream approximation the notion "tem-

perature" stands for a convenient parametrization of the energy density. Its initial and final values are calculated via $T_0 = (T_c \frac{dN_c/dy}{3\pi R^2 \tau_0})^{1/4}$. The $q_\perp$ dependence of the dilepton spectrum at transverse mass $M_\perp = 2.6$ GeV according to Eq. (6) is displayed in Fig. 1. We have chosen a set of unique initial parameters in line with the estimates for Au + Au collisions at RHIC [15] $\tau_0 = 0.13$ fm/c, charged particle rapidity density $dN_c/dy = 1000$, as well as $K = 1$ GeV^2 and $p_\perp^* = 1.25$ GeV. The transverse radius is chosen as 5 fm, and as breakup density parametrization we use $T_c = 200$ MeV, which is thought to be somewhat above the confining transition, where our kinetics no longer apply. The value of $M_\perp$ is just in the continuum region below the J/ψ, where sufficiently many pairs are to be observed. We consider midrapidity pairs with $Y = 0$, for which the boost invariance should be a good approximation (the Y distribution is analyzed in Ref. [22]).

Let us first consider the case of the soft initial distribution. One observes for the strongly anisotropic parton distribution function (5a) an approximate scaling within accuracy of factor of 2. Clearly the yield exceeds that of a quark-gluon plasma which could be formed afterwards, if thermalization processes are efficient enough. A change of the slope parameter K from 1 to 1.5 GeV^2 does not change the spectrum noticeably, while lower values of K reduce the averaged yield, but leave the form of the spectrum nearly unchanged.

As a measure of the quality of the scaling one can use, as in Ref. [7], the ratio $\mathcal{R} = \frac{dN/dM_\perp^2 dq_\perp^2 dY(q_\perp=2\text{GeV})}{dN/dM_\perp^2 dq_\perp^2 dY(q_\perp=0\text{GeV})}$ at fixed $M_\perp = 2.6$ GeV. For the quark-gluon plasma ideally one has $\mathcal{R} = 1$. In Ref. [7] a value $\mathcal{R} < 3$ is considered as a plausible signal of the plasma. In the present example one gets $\mathcal{R} \simeq 2/3$ independent of dN_c/dy. This result should be considered in conjunction with the analysis of Ref. [11] where also the Drell-Yan yield is found to display such approximate scaling. One might therefore conjecture that for a certain class of initial parton distributions and evolution scenarios an approximate $M_\perp$ scaling appears. (Unfortunately, we did not find a general proof; without specifying the initial distribution, definite conclusions do not seem possible.) Hence an approximate scaling $\mathcal{R} \sim 1$ can no longer be considered a unique signal of a thermalized quark-gluon plasma.

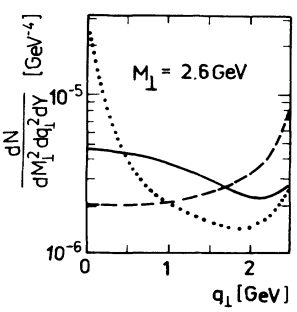

FIG. 1. The transverse momentum dependence of the dilepton spectrum from free-streaming parton matter at $M_\perp = 2.6$ GeV according to Eq. (6) [full, dotted, and dashed lines for (a), (b), and (c), respectively].

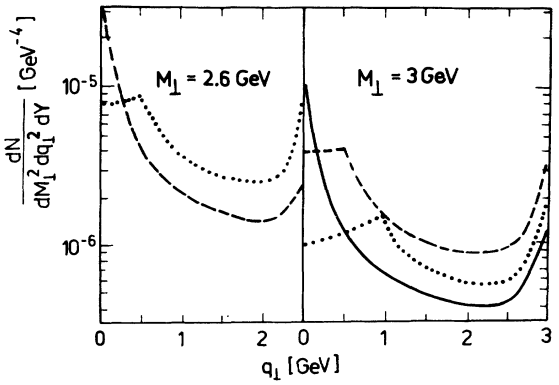

FIG. 2. Transverse momentum dependence of dilepton spectrum according to Eq. (6b) for $M_\perp = 2.6$ (left panel) and 3 (right panel) GeV, and $p_\perp^* = 1$, 1.25, and 1.45 GeV (dotted, dashed, and full lines).

A similar good approximate scaling ($\mathcal{R} \simeq 1.5$, we focus on the region of a not too large $q_\perp$) as in the previous example is observed for the initially thermalized parton distribution (5c), see Fig. 1. This is to be expected since the main contributions of large-M pairs come from the early stage wherein the distribution does not evolve too far from the thermalized state.

The initial distribution (5b) represents an example which displays a stronger scaling violation ($\mathcal{R} \simeq 0.045$). Here one has introduced the essentially additional low-momentum cutoff parameter $p_\perp^* = 1.45$ GeV. A very similar form of the transverse momentum spectrum has also been found in Ref. [17]. One might therefore conclude that the initial parton distributions are similar, i.e., of

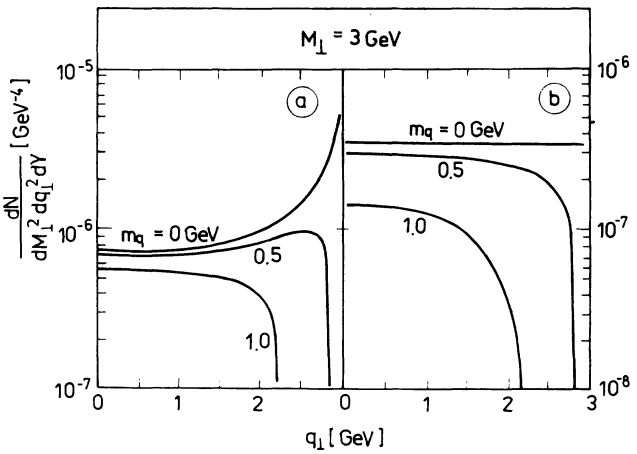

FIG. 3. The $q_\perp$ dependence of the dilepton spectrum for an initially thermalized quark-gluon plasma with finite quark masses; (a) subsequent free-stream evolution, (b) local thermalization is kept during the subsequent evolution. Initial values are as in Fig. 1 for (a), and $T_0 = 333$ MeV, $\tau_0 = 1$ fm/c [24] for (b). When using $T_0 = 536$ MeV, $\tau_0 = 0.13$ fm/c [15] in (b) the curves are shifted up by a factor of 1.5.

the power-law form which emerges by using the perturbative QCD cross sections for parton scatterings in the minijet scenario. Physically this scaling violation is intimately related to the restriction of the phase space due to the cutoff. In Fig. 2 several spectra are displayed for various values of the cutoff. (Notice that our curve for $M_\perp = 3$ GeV with $p_\perp^* = 1.45$ GeV coincides with the result displayed in Fig. 2(a) in Ref. [17].)

A larger value of $p_\perp^*$ is seen to cause a stronger scaling violation. The appearance of the local maximum (which also is seen in Fig. 3(b) of Ref. [17] for early times) is caused by the kinematical boundary $q_\perp = M_\perp - 2p_\perp^*$ which separates phase-space regions in which the created dileptons, at given $M_\perp$ and $q_\perp$, feel the phase-space restriction by the cutoff or not, see the definition of L in Eq. (6b). According to the findings of Ref. [17] in the subsequent evolution softer partons are also produced which then wash out this local low-$q_\perp$ peak. This form of the spectrum is rather different from the one resulting from a hadron gas and a possible mixed phase, where the yield continuously and steeply increases with increasing $q_\perp$ up to $q_\perp \approx (M_\perp^2 - m_\rho^2)^{1/2}$ (m_ρ is the ρ mass) [8]. Therefore, the shape of the $q_\perp$ spectrum is considered useful for the diagnostic of parton matter formation.

From Eq. (6) one easily deduces that in the small-$q_\perp$ region the rate obeys an $M_\perp$ dependence as

$$\frac{dN}{dM_\perp^2 dq_\perp^2 dY}\Big|_{q_\perp=0} \propto \begin{cases} \exp\left(-\frac{M_\perp^2}{2K}\right), & \text{(7a)} \\ M_\perp^{-2l}, & \text{(7b)} \\ K_1^2\left(\frac{M_\perp}{2T_0}\right) \approx M_\perp^{-1}\exp\left(-\frac{M_\perp}{T_0}\right). & \text{(7c)} \end{cases}$$

Equation (7) shows how the parameters K, l, T_0 determine basically the $M_\perp$ spectrum.

IV. INFLUENCE OF RELAXATION PROCESSES

In Ref. [13] finite relaxation times are studied. We apply this formalism to study numerically the effect of thermalization during the time evolution of f. This replaces eq. (4) by a more realistic one (for details we refer the reader to Refs. [13,14]). In the case of f_0 (5a) we find for $K = 0.6$–1.5 GeV^2 values of $\mathcal{R} \simeq 0.7$ (as in the free-stream approximation), rather independent of the relaxation time $\tau_{\rm rel} = 0.05$–1 fm/c. Only for very large values of $K = 2.4$ GeV^2 (which seem to be too large for RHIC, but might apply at the CERN Large Hadron Collider) $\mathcal{R}$ changes from 0.7 to 1 when varying $\tau_{\rm rel}$ from 1 to 0.05 fm/c. These findings hold in the region $M_\perp = 2.6$ GeV up to large values, say 5 GeV.

Such an outcome is quite expected since such large-$M_\perp$ pairs are created in early stages; the relaxation process in the subsequent evolution does not change too much this early spectrum. Naturally one realizes that the relaxation process improves the scaling, since it drives the parton system towards local thermalization. We therefore conclude that the free-stream studies of the previous section are also not changed basically when allowing for thermalization processes for the initial distributions (5a) and (5b).

V. FINITE QUARK MASSES

The above presented results employ vanishing quark masses, i.e., $m_q = 0$. The interpretation of lattice QCD calculations, however, point to finite effective parton masses [14,23]. Also perturbative QCD analysis at finite temperature leads to substantial thermal masses in the order of magnitude of the temperature. We have studied this effect for a thermalized quark-gluon plasma with constant quark mass. The rate is in this case

$$\frac{dN}{dM_\perp^2 dq_\perp^2 dY} = \frac{5\alpha^2 R^2}{72\pi^2}\left(1 - \frac{4m_q^2}{M^2}\right)^{3/2} \frac{6(T_0^3\tau_0)^2}{M_\perp^6} \times \left[H_0\left(\frac{M_\perp}{T_c}\right) - H_0\left(\frac{M_\perp}{T_0}\right)\right] \qquad (8)$$

$[H_0(x) = -x^3(x^2+8)K_3(x)]$. As seen in Fig. 3(b) a finite quark mass in the order of magnitude of 500 MeV already causes a noticeable scaling violation by reducing the rate near the kinematical boundary at large $q_\perp$. In our above examples with $m_q = 0$ the rate increases at large $q_\perp$ (because one enters there the small M region where the yield increases). Phase-space exhaustion by the finite quark mass oppositely reduces then the rate. This is seen in Fig. 3(a) for the initial distribution (5c), for which the rate reads as (6c), however, with I to be replaced by $\bar{I}$,

$$\bar{I} = \sqrt{1 - \frac{4m_q^2}{M_\perp^2 - q_\perp^2}} \int_{x_-}^{x_+} \frac{dx x K_1\left(\frac{Mx}{T_0}\right) K_1\left(\frac{M}{T_0}[\frac{M_\perp}{M} - x]\right)}{\sqrt{x(\frac{M_\perp}{M} - x) - \frac{1}{4} - \frac{m_q^2}{M^2}\frac{q_\perp^2}{M^2}}}, \qquad (9)$$

$$x_\pm = \frac{1}{2}\left(\frac{M_\perp}{M} \pm \frac{q_\perp}{M}\sqrt{1 - \frac{4m_q^2}{M^2}}\right).$$

For suitable quark masses the scaling in the latter case is restored partially at not too large values of $q_\perp$, i.e., $\mathcal{R}$ shifts towards 1.

This effect of reducing the yield by finite quark mass at large $q_\perp$ might be experimentally searched for to get valuable information of whether the finite quark masses become operative. It should be noticed, however, that large $q_\perp$ correspond to small values of M, where other sources are expected to dominate. In particular the contributions from the ρ resonance-dominated $\pi\pi$ annihilation in the hadron and possible mixed phase show up there [7,8]. Their strength depends on details of the late transverse expansion and dynamics of the confinement transition. These items need further investigation.

VI. SUMMARY

In summary, we analyze the transverse momentum dependence of dileptons at fixed transverse mass. We follow the suggestions of earlier work which considers the $M_\perp$ scaling property of the dilepton yield in case of a locally thermalized quark-gluon plasma, and extend it to preequilibrium states and finite quark masses. We find that under certain conditions approximate scaling also persists for off-equilibrium parton matter, while additional essential parameters in the parton source description cause violation of the scaling. As in the dynamical parton cascade model we get scaling violation of $\mathcal{R}^{-1} \approx 20$ for a semihard, minijet-produced initial distribution. The strength of violation of course depends on the low-momentum cutoff. Other initial distributions, as, e.g., produced by a soft Schwinger mechanism, display better scaling $\mathcal{R}^{-1} \approx 2$. We suggest that an experimental study of the scaling properties at RHIC is useful for clues on the early parton evolution, and the $q_\perp$ dependence might provide an indication as to which mechanism of initial secondary parton production is operative. Since the scaling violation for the hadron gas is much stronger ($\mathcal{R} > 30$), the approximate scaling property $\mathcal{R} < 3$ and the shape of the $q_\perp$ spectrum are suitable for identifying a parton source of the dileptons. Whether the dileptons are simply of Drell-Yan origin or from an evolving parton gas with efficient secondary collisions might be decided as proposed in Ref. [25].

ACKNOWLEDGMENTS

O.P.P. thanks the nuclear theory group in Research Center Rossendorf for the warm hospitality. Useful discussions with M. Asakawa, K. Geiger, C. Ko, B. Müller, E. Shuryak, D. Seibert, and G. Zinovjev are gratefully acknowledged. The work is supported by BMFT under Grant No. 06 DR 107.

[1] E.L. Feinberg, Nuovo Cimento **34A**, 391 (1976).
[2] E. Shuryak, Phys. Lett. **78B**, 150 (1978).
[3] P.V. Ruuskanen, in *Quark Gluon Plasma*, edited by R. Hwa (World Scientific, Signapore, 1990), p. 519, and references therein.
[4] O.V. Zhirov, Yad. Fiz. **30**, 1098 (1979).
[5] L. McLerran and T. Toimela, Phys. Rev. D **31**, 545 (1985).
[6] R. Hwa and K. Kajantie, Phys. Rev. D **32**, 1109 (1985).
[7] M. Asakawa, C.M. Ko, and P. Levai, Phys. Rev. Lett. **70**, 398 (1993).
[8] K. Kajantie, M. Kataja, L. McLerran, and P.V. Ruuskanen, Phys. Rev. D **34**, 811 (1986).
[9] V. Emeljanov and Yu. Nikitin, Yad. Fiz. **51**, 1693 (1990).
[10] A. Białas and J.P. Blaizot, Phys. Rev. D **32**, 2954 (1985), and references therein.
[11] M. Asakawa and T. Matsui, Phys. Rev. D **43**, 287 (1991).
[12] K. Kajantie and P.V. Ruuskanen, Z. Phys. C **44**, 167 (1989).
[13] B. Kämpfer and O.P. Pavlenko, Phys. Lett. B **289**, 127 (1992).
[14] B. Kämpfer and O.P. Pavlenko, Report FZR-93-16 (unpublished); Nucl. Phys. **A566**, 351c (1994).
[15] J. Kapusta, L. McLerran, and D.K. Srivastava, Phys. Lett. B **283**, 145 (1992).
[16] K. Geiger and J. Kapusta, Phys. Rev. Lett. **70**, 1920 (1993).
[17] K. Geiger, Report NUC-MINN-93/10-T, 1993; Phys. Rev. Lett. **71**, 3075 (1993).
[18] E. Shuryak and L. Xiong, Phys. Rev. Lett. **70**, 2241 (1993).
[19] G. Baym, Phys. Lett. **138B**, 18 (1984).
[20] K. Kajantie, P.V. Landshoff, and J. Lindfors, Phys. Rev. Lett. **59**, 2527 (1987); K.J. Eskola, K. Kajantie, and J. Lindfors, Nucl. Phys. **B323**, 37 (1989).
[21] T. Biró, B. Müller, E. van Dorn, M. Thoma, and X.N. Wang, Phys. Rev. C **48**, 1275 (1993); K.J. Eskola and X.N. Wang, Report LBL-34156 (1993); X.N. Wang and M. Gyulassy, Phys. Rev. D **44**, 3501 (1991).
[22] R. Vogt, B.V. Jacak, P.L. McGaughey, and P.V. Ruuskanen, Report No. GSI-93-65.
[23] V. Golovishnin and H. Satz, poster T43 presented at Quark Matter '93 (Borlänge, Sweden, 1993).
[24] H. Satz, Nucl. Phys. **A544**, 371c (1992).
[25] B. Kämpfer and O.P. Pavlenko, Phys. Lett. B **255**, 503 (1991).